

## QUENCHING OF THE FLUORESCENCE OF NO<sub>2</sub>

SILVIA BRASLAVSKY and JULIAN HEICKLEN

*Department of Chemistry and Ionosphere Research Laboratory, The Pennsylvania State University, University Park, Pa. 16802 (U.S.A.)*

(Received May 2, 1972; in revised form July 20, 1972)

### SUMMARY

The fluorescence yield of NO<sub>2</sub> was monitored at 25°C with incident wavelengths of 4047, 4358, and 4800 Å at fluorescence wavelengths of 4860, 5577, and 6300 Å. The NO<sub>2</sub> pressure was varied between 0.004 and 0.080 Torr. Measurements were taken both in the absence of foreign gases and in the presence of up to 30 Torr He, N<sub>2</sub>, and O<sub>2</sub> at each NO<sub>2</sub> pressure. In the absence of foreign gases, the self quenching follows a Stern–Volmer quenching mechanism, but foreign-gas quenching shows marked deviations from this mechanism. Both from lifetime and kinetic considerations, it is argued that the electronic state formed by absorption of the radiation cannot be the emitting state. Emission occurs from several vibrational levels of the emitting state, the various vibrational levels being formed by collisional cascade reactions. The appropriate quenching rate constant ratios have been measured and tabulated. Even the two electronic state mechanism is insufficient to explain all the observations.

---

### INTRODUCTION

The fluorescence of gaseous NO<sub>2</sub> has been the subject of several studies, with neither the experimental results nor the explanations always in agreement. In 1929 Norrish<sup>1</sup> reported a dependence of the emission spectrum on the wavelength of the incident radiation,  $\lambda_i$ . This result was not supported by the subsequent work of Neuberger and Duncan<sup>2</sup>. These authors observed the same radiative lifetime of  $\tau = 4.4 \times 10^{-5}$  sec for three different  $\lambda_i$  (3950, 4300, and 4650 Å). This value was more than two orders of magnitude larger than that of  $2.6 \times 10^{-7}$  sec calculated by the same authors from the integrated extinction coefficient using the absorption coefficient curves of Hall and Blacet<sup>3</sup> and of Dixon<sup>4</sup>. To account for the anomaly, Neuberger and Duncan proposed the participation of two electronic states, one absorbing and the other emitting the radiation.

In 1966, Douglas<sup>5</sup> proposed four different mechanisms, which may account for the anomalous lifetimes found not only in the NO<sub>2</sub> case, but also in the SO<sub>2</sub> and Cs<sub>2</sub> cases. In all four mechanisms only one excited electronic state was considered and, according to the author, the most likely explanation for the long radiative lifetime of NO<sub>2</sub> is the interaction of the excited electronic state with the upper vibrational levels of the ground state.

As for the quenching of the fluorescence, Baxter<sup>6</sup> measured relative quenching efficiencies of several gases in 1930. In 1965 Myers *et al.*<sup>7</sup> studied the relative efficiencies of 13 different gases. These authors found linearity in the Stern–Volmer plots for pressures of NO<sub>2</sub> ranging from 5 to 30 mTorr. They did not report the range of pressures of added gases used in the experiments. They also found a dependence of the Stern–Volmer quenching constants on the wavelengths of both the exciting and fluorescent radiation. Furthermore the fluorescence spectrum showed a red shift at high quenching pressures, indicating that some vibrational quenching was occurring prior to fluorescence.

In a more recent paper, Keyser *et al.*<sup>8</sup> measured the radiative lifetime of the excited NO<sub>2</sub> using a phase shift method. In this case they found a curvature in the self-quenching Stern–Volmer plots at low NO<sub>2</sub> pressures, the curvature increasing with the separation between the incident wavelength,  $\lambda_i$ , and the emitted wavelength,  $\lambda_f$ . To explain their results they suggested a cascade model with stepwise vibrational deactivation in a single excited electronic state, concurrent with its electronic and radiative deactivation. They found the radiative lifetime to be  $5.5 \times 10^{-5}$  sec independent of exciting wavelength. They accepted the Douglas model to explain the long lifetime, and thus excluded the participation of more than one electronically excited state.

Schwartz and Johnston<sup>9</sup> had also examined the radiative lifetime by a phase shift method and had found similar results, the only difference being a slight dependence of the radiative lifetime ( $5.5 \times 10^{-5}$  to  $9 \times 10^{-5}$  sec) on the incident radiation. Schwartz and Johnston also accepted the single electronic state mechanism for absorption and emission.

In 1969, Sakurai and Broida<sup>10</sup> studied the fluorescence of NO<sub>2</sub> using several different incident wavelengths from a laser source. They found that the extinction coefficients were proportional to the NO<sub>2</sub> pressure at all wavelengths. They argued that the earlier measurements<sup>3,4</sup> of large extinction coefficients were unreliable for this reason, as well as possible failure to correct for instrument slitwidth, and estimated the lifetime, based on the integrated absorption coefficient to be about  $10^{-5}$  sec, in approximate agreement with the radiative lifetime. They also accepted the one electronic state mechanism and explained the effect of NO<sub>2</sub> pressure on the fluorescence intensity in terms of vibrational deactivation.

In 1971, calculations on the electronic structure of the ground and excited states of NO<sub>2</sub> were done by two different research groups, Fink<sup>11</sup> in California and Gangi and Burnelle<sup>12,13</sup> in New York. Fink concluded that the explanation of the

visible spectrum of NO<sub>2</sub> requires a treatment which considers the simultaneous perturbation of the rotational-vibrational levels of at least three different electronic states.

Gangi and Burnelle<sup>13</sup> suggest that absorption of light at wavelengths between 4000 and 6000 Å is mainly from the ground <sup>2</sup>A<sub>1</sub> state to the second excited <sup>2</sup>B<sub>2</sub> state. They compute the radiative lifetime for the unperturbed <sup>2</sup>B<sub>2</sub> state to be  $0.1248 \times 10^{-6}$  sec, similar to the value computed by Neuberger and Duncan<sup>2</sup>. Thus if emission is from <sup>2</sup>B<sub>2</sub>, it must be mixed with lower electronic states as suggested by Douglas<sup>5</sup> to account for the long lifetime. Gangi and Burnelle accept this hypothesis, but point out that <sup>2</sup>B<sub>2</sub> could interconvert to the lower lying <sup>2</sup>B<sub>1</sub> state, and that some emission could be coming from that state. Furthermore for incident radiation above ~6000 Å, there is insufficient energy to populate <sup>2</sup>B<sub>2</sub>, and <sup>2</sup>B<sub>1</sub> presumably is being excited directly.

There is direct experimental evidence relating to the symmetry of the absorbing and emitting electronic states. Douglas and Huber<sup>14</sup> have shown that the <sup>2</sup>B<sub>1</sub> state is responsible for the discrete absorption bands in the region from 3700 to 4600 Å, though Sackett and Yardley<sup>15</sup> have shown that the <sup>2</sup>B<sub>2</sub> state also absorbs at 4515–4605 Å, and that this absorption is more pronounced than that to <sup>2</sup>B<sub>1</sub>. Abe *et al.*<sup>16</sup> demonstrated that emission is from a single vibrational level of the <sup>2</sup>B<sub>2</sub> state when excitation is at 5145 Å.

We present in this paper the results of the quenching of NO<sub>2</sub> fluorescence by itself as well as by He, N<sub>2</sub>, and O<sub>2</sub>. The incident wavelengths used were 4047, 4358, and 4800 Å. Emission was monitored at 4860, 5577, and 6300 Å. Contrary to the findings in Kaufman's laboratory<sup>7,8</sup>, we find marked deviation from linearity of the Stern-Volmer quenching plots with the added gases. Presumably this is because we have extended the pressure range of the experiments. As a result we feel that our findings preclude the possibility that the emitting and absorbing states are the same.

## EXPERIMENTAL

A conventional fluorescence system was used consisting of a mercury free, grease free, high vacuum line, a dibutyl phthalate manometer, several calibrated volumes providing known expansion ratios, and a fluorescence cell. The T-shaped vessel, made from 7 cm i.d. Pyrex tubing, was 7 cm long, with a 2.45 cm side arm extending 1 cm from the middle of the principal axis, and two 2.45 cm diameter openings, extending 0.5 cm from the ends. Three 2.45 cm diameter sapphire windows (Harshaw Optical Crystals) were sealed with epoxy resin to the three openings. Two different lamps were used, a 200 W high pressure mercury arc (Illumination Ind. Inc.) for the 4047 and 4358 Å radiation, and a Hanovia 418C-9, 800 W high pressure xenon compact arc for the 4800 Å radiation. In every case the light was collimated to a 0.5 cm cross-section parallel beam, filtered through the

appropriate interference filter and then collimated to a conic beam by means of a 10 cm focal length quartz lens placed in front of the reaction vessel.

The following interference filters were used for the exciting radiation: 4050/50A (Thin film products) and 4360/100A and 4800/100A (Baird Atomic, Inc.). When the high pressure Xe arc was used a 10 cm long, 5 cm i.d. quartz vessel filled with water was used to cool the beam, in order to protect the interference filter.

The intensity of the incident beam was monitored with an RCA 935 photodiode placed after the reaction vessel, and a 1 mV recorder (Texas Instruments) to measure the voltage drop across a known variable resistor. Fluorescence was observed through the side arm of the cell. The following combinations of interference filters and Corning sharp cutoff filters were used in monitoring the emitted radiation at the different wavelengths, to reduce the background light from the exciting source.

4860/50A: Baird Atomic, Inc. interference filter plus Corning CS 3-72.

5577/15A: Thin Film Prod. interference filter plus either Corning CS 3-73 when  $\lambda_i$  was 4047 Å, or Corning CS 3-70 when  $\lambda_i$  was 4358 Å.

6300/15A: Thin Film Prod. interference filter plus Corning CS 2-63.

The fluorescence signal was detected with a non-cooled EMI 9558B photomultiplier. This tube has an S-20 response cathode, and was operated at 1500 V by means of a 402M John Fluke Power Supply.

The photomultiplier was wrapped with aluminium foil and then with a Mu Metal Shield which was connected to the cathode terminal in order to keep it at cathode potential to reduce the erratic noise. The photomultiplier was operated at a gain of  $2 \times 10^6$  which gave a dark current of  $3 \times 10^{-11}$  A. The output was amplified with a Keithley 410A picoammeter, and displayed on a strip chart recorder (Texas Instruments). Fluorescence signals were corrected for variations of the intensity of the exciting beam, and for the background signal due to scattered light.

The  $\text{NO}_2$  (Matheson Co.) was purified by mixing it with  $\text{O}_2$  and then distilling it through a  $-80^\circ\text{C}$  (acetone) slush. The purified solid was completely white and it was kept covered with black felt at all times. The purity was checked by examining the color of the solid before each run. When 4047 Å radiation was incident, only short exposures were used to minimize photodecomposition.

The desired pressures of  $\text{NO}_2$  (about 0.004 to 0.08 Torr) were obtained by expansion in known volumes from measured pressures with the oil manometer. Corrections were made for the  $\text{NO}_2\text{-N}_2\text{O}_4$  equilibrium when necessary.

$\text{N}_2$  (Matheson Co., Prep. Grade),  $\text{O}_2$  (Matheson Co., Extra Dry) and He (Matheson Co., High Purity) were used without further purification.

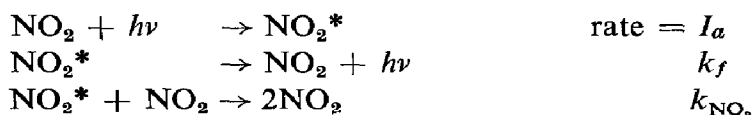
## RESULTS

$\text{NO}_2$  was excited by monochromatic steady illumination at three wavelengths. For each incident wavelength,  $\lambda_i$ , the relative intensity of the fluorescence

was determined at different wavelengths,  $\lambda_f$ , as a function of NO<sub>2</sub> pressure. The relative incident intensity was also monitored, and the ratio  $Q$ , of relative fluorescence intensity,  $I_f$ , to relative incident intensity,  $I_o$ , was tabulated.

In order to keep the absorbed intensity,  $I_a$ , small compared to  $I_o$ , pressures of NO<sub>2</sub> < 0.080 Torr were used. The lower limit of NO<sub>2</sub> pressure used was 0.004 Torr, in order to avoid the deviation from Stern–Volmer quenching observed by others<sup>8, 9</sup> at lower pressures.

The simple Stern–Volmer mechanism involves excitation to a single state followed by either fluorescence or collisional deactivation.



Since low NO<sub>2</sub> pressures were used,  $I_a = \epsilon I_o [\text{NO}_2]$ , where  $\epsilon$  is the extinction coefficient. Furthermore let  $Q \equiv I_f/I_o$ , so that the simple mechanism leads to the expression:

$$[\text{NO}_2]/Q_o = \epsilon^{-1}(1 + k_{\text{NO}_2}[\text{NO}_2]/k_f) \tag{I}$$

where the subscript “o” on  $Q$  indicates the absence of added foreign gases.

Figures 1 and 2 show plots of  $[\text{NO}_2]/Q_o$  vs.  $[\text{NO}_2]$  for the seven combinations of incident and fluorescence wavelengths studied. In all cases the data are well fitted by straight lines, in agreement with the findings of others<sup>8, 9</sup> for  $[\text{NO}_2] > 0.005$  Torr.

In the presence of a foreign gas, M, an additional reaction must be added to the simple Stern–Volmer mechanism:

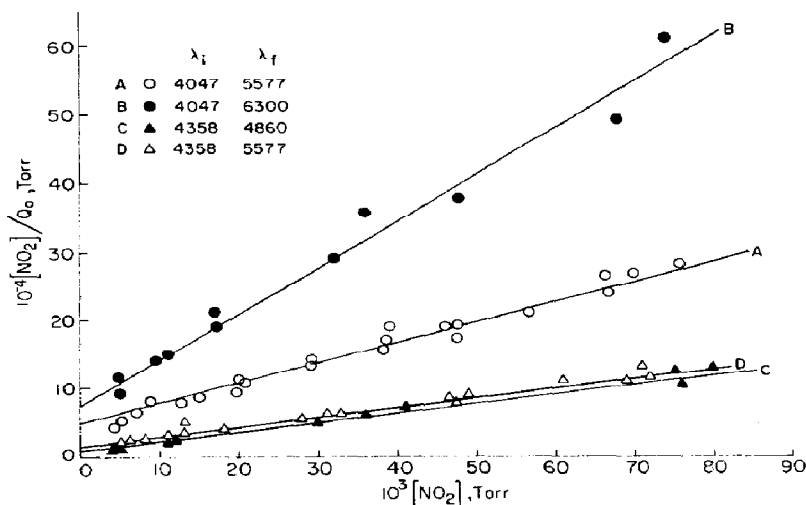


Fig. 1. Plots of  $[\text{NO}_2]/Q_o$  vs.  $[\text{NO}_2]$  for the emission of NO<sub>2</sub> at 25°C at various incident and fluorescence wavelengths.

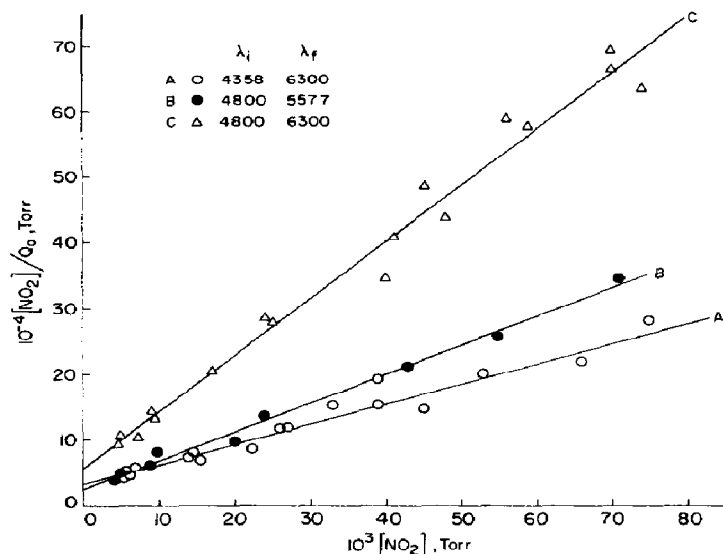


Fig. 2. Plots of  $[\text{NO}_2]/Q_0$  vs.  $[\text{NO}_2]$  for the emission of  $\text{NO}_2$  at  $25^\circ\text{C}$  at various incident and fluorescence wavelengths.

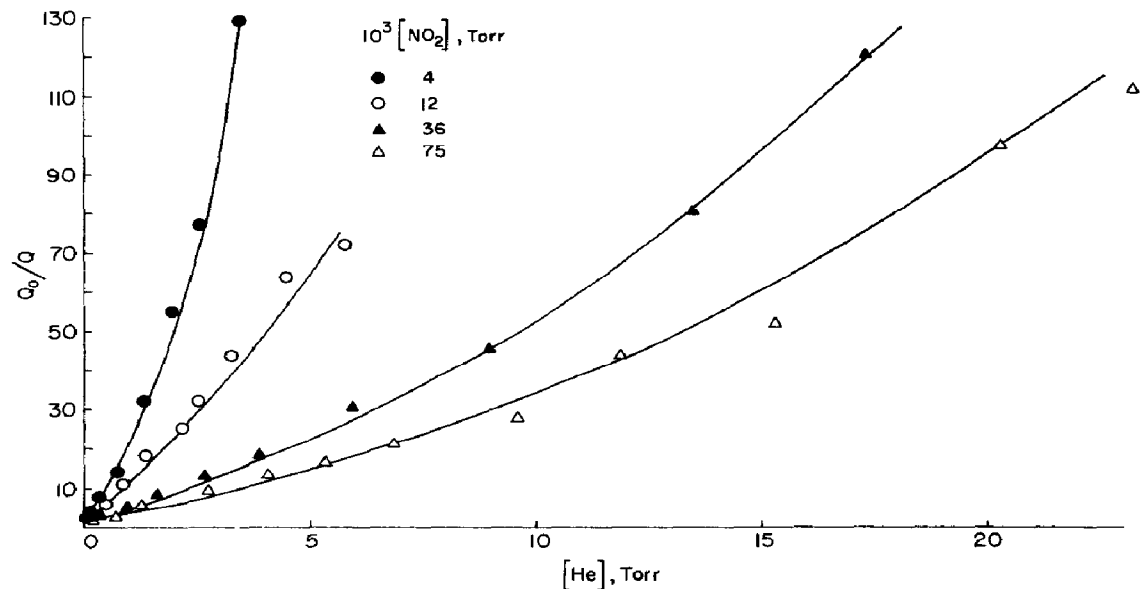


Fig. 3. Plots of  $Q_0/Q$  vs.  $[\text{He}]$  at various  $\text{NO}_2$  pressures for the emission of  $\text{NO}_2$  in the presence of He at  $25^\circ\text{C}$  with  $\lambda_i = 4358 \text{ \AA}$  and  $\lambda_f = 4800 \text{ \AA}$ .



The effect of this reaction on the Stern–Volmer relative fluorescence yield is given by the expression:

$$Q_0/Q = 1 + k_{\text{M}}[\text{M}]/(k_f + k_{\text{NO}_2}[\text{NO}_2]) \quad (\text{II})$$

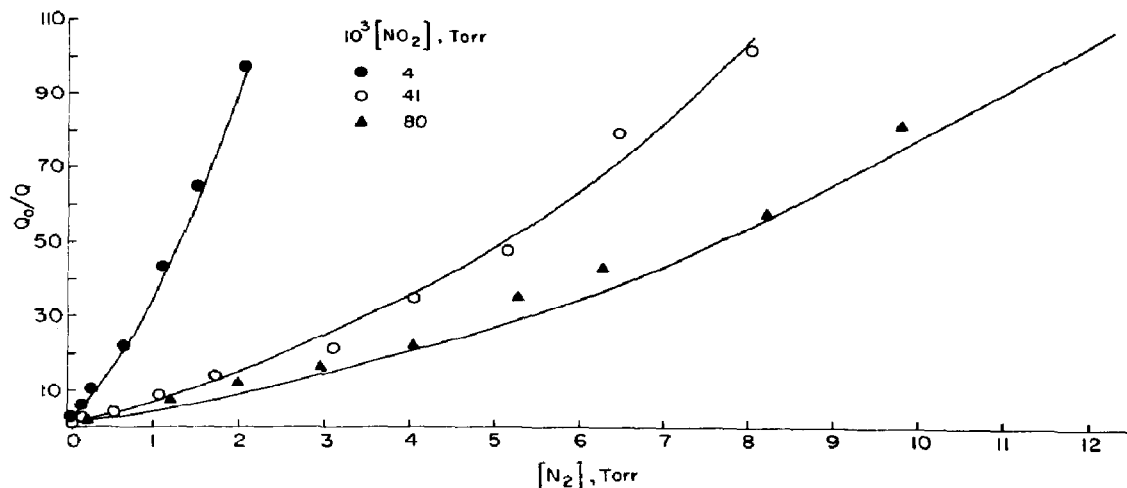


Fig. 4. Plots of  $Q_0/Q$  vs.  $[N_2]$  at various NO<sub>2</sub> pressures for the emission of NO<sub>2</sub> in the presence of N<sub>2</sub> at 25°C with  $\lambda_i = 4358 \text{ \AA}$  and  $\lambda_f = 4800 \text{ \AA}$ .

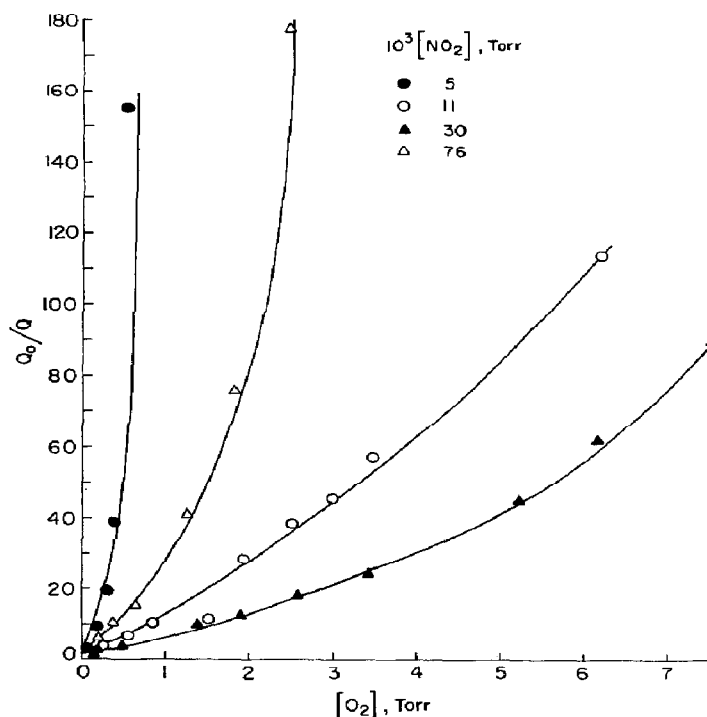


Fig. 5. Plots of  $Q_0/Q$  vs.  $[O_2]$  at various NO<sub>2</sub> pressures for the emission of NO<sub>2</sub> in the presence of O<sub>2</sub> at 25°C with  $\lambda_i = 4358 \text{ \AA}$  and  $\lambda_f = 4800 \text{ \AA}$ .

where again  $Q_0$  is the relative fluorescence yield in the absence of M and  $Q$  is the relative fluorescence yield at the same NO<sub>2</sub> pressure in the presence of the foreign gas.

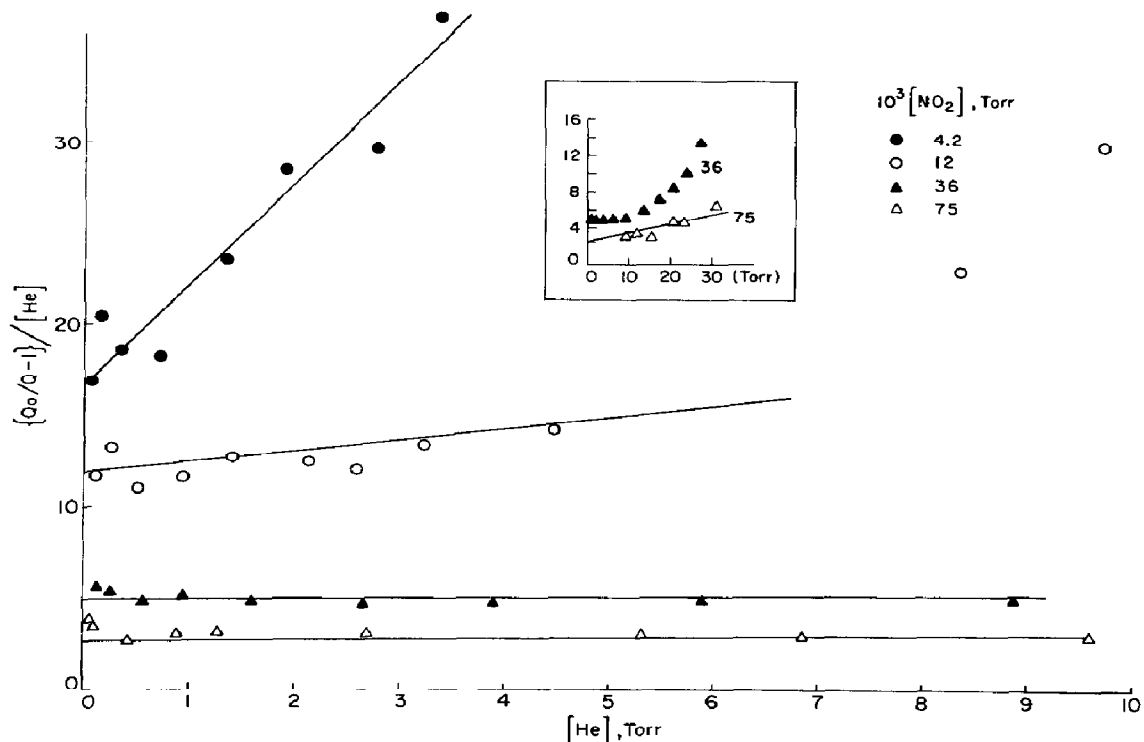


Fig. 6. Plots of  $(Q_o/Q-1)/[He]$  vs.  $[He]$  at various  $NO_2$  pressures for the emission of  $NO_2$  in the presence of He at  $25^\circ C$  with  $\lambda_i = 4358 \text{ \AA}$  and  $\lambda_f = 4800 \text{ \AA}$ .

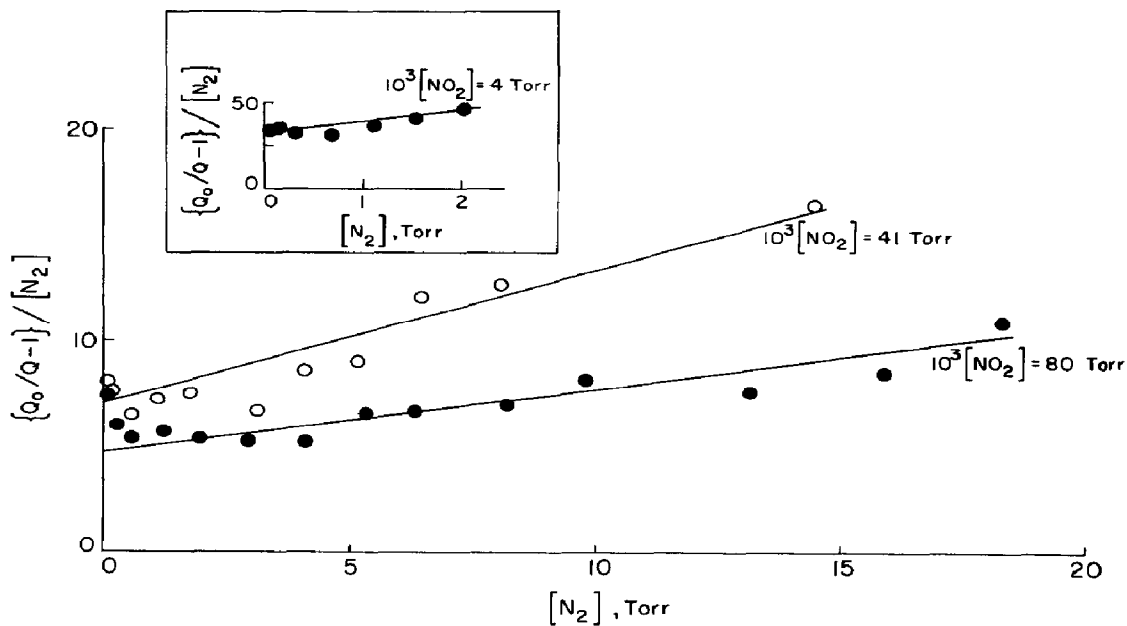


Fig. 7. Plots of  $(Q_o/Q-1)/[N_2]$  vs.  $[N_2]$  at various  $NO_2$  pressures for the emission of  $NO_2$  in the presence of  $N_2$  at  $25^\circ C$  with  $\lambda_i = 4358 \text{ \AA}$  and  $\lambda_f = 4800 \text{ \AA}$ .

Equation (II) predicts that a plot of  $Q_o/Q$  vs.  $[M]$  should be linear at constant  $[\text{NO}_2]$  for any incident and fluorescence wavelengths. Such plots are shown for  $\lambda_i = 4358 \text{ \AA}$  and  $\lambda_f = 4860 \text{ \AA}$  for  $M = \text{He}, \text{N}_2,$  and  $\text{O}_2$ , respectively, in Figs. 3, 4 and 5. It is clear that in all cases the plots show marked curvature in the upward direction. Similar plots (not shown) for all the other incident and fluorescence wavelengths show the same curvature. Our results are in apparent disagreement with those of Myers *et al.*<sup>7</sup> who did not indicate any deviation from linearity, though they did not report either their data or their pressure range. Presumably the discrepancy can be attributed to the possibility that we have greatly extended the pressure range of the quenching gases.

We find that straight-line plots can be obtained for the function

$$(Q_o/Q-1)/[M] = \alpha + \beta[M] \quad (\text{III})$$

where  $\alpha$  and  $\beta$  are functions of  $\lambda_i, \lambda_f,$  and  $[\text{NO}_2]$ . Plots of  $(Q_o/Q-1)/[M]$  vs.  $[M]$  are shown for He, N<sub>2</sub>, and O<sub>2</sub>, respectively, in Figs. 6, 7 and 8 for  $\lambda_i = 4358 \text{ \AA}$  and  $\lambda_f = 4860 \text{ \AA}$ . Only for  $[\text{NO}_2] \geq 0.036 \text{ Torr}$  and  $M = \text{He}$  is there any deviation from linearity, and then only above 10 Torr of He. Our experimental uncertainty

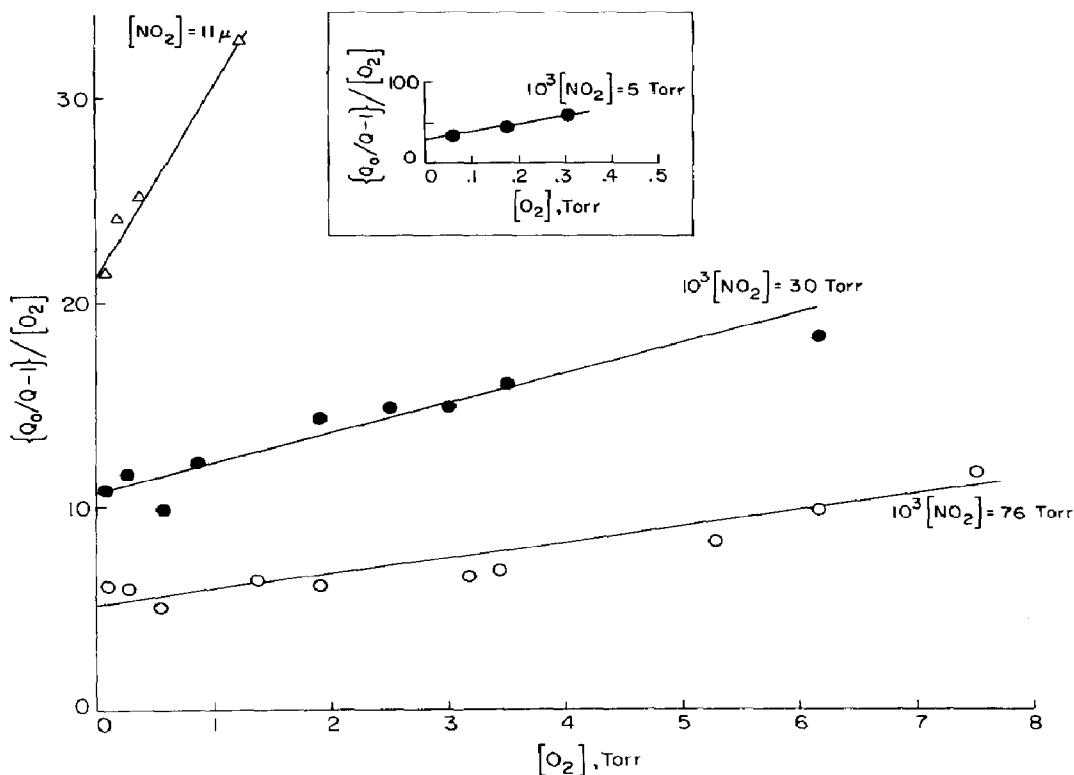


Fig. 8. Plots of  $(Q_o/Q-1)/[O_2]$  vs.  $[O_2]$  at various  $\text{NO}_2$  pressures for the emission of  $\text{NO}_2$  in the presence of  $\text{O}_2$  at  $25^\circ \text{C}$  with  $\lambda_i = 4358 \text{ \AA}$  and  $\lambda_f = 4800 \text{ \AA}$ .

in this range is quite large, and perhaps this deviation is an experimental artifact. In any event, at the other wavelengths of incidence and emission, none of the plots (not shown) deviated from linearity over the same pressure ranges (up to 10–30 Torr of M). Values of  $\alpha$  and  $\beta$  are listed in Table I. Their dependence on  $[\text{NO}_2]$  is apparent, the values of both  $\alpha$  and  $\beta$  decreasing as  $[\text{NO}_2]$  increases.

TABLE I  
VALUES OF  $\alpha$  AND  $\beta$  EQN. (III)

$10^3[\text{NO}_2]$ (Torr)	$\alpha$ (Torr <sup>-1</sup> )	$\beta$ (Torr <sup>-2</sup> )	$\beta/\alpha$ (Torr <sup>-1</sup> )
$\lambda_i = 4047 \text{ \AA}, \lambda_f = 5577 \text{ \AA}, \text{M} = \text{He}$			
8.7	5.5		
21.5	4.8	6	1.25
39.2	3.7	2.82	0.76
46	2.9	0.67	0.23
56.7	2.7	0.33	0.122
70	2.3	0.28	0.122
$\lambda_i = 4047 \text{ \AA}, \lambda_f = 5577 \text{ \AA}, \text{M} = \text{N}_2$			
5.3	9.2	15.25	1.66
19.4	8.1	3.14	0.39
38.2	6.5	1.56	0.24
47.5	5.4	1.44	0.27
66.8	3.4	1.08	0.32
75.7	3.2	0.88	0.28
$\lambda_i = 4047 \text{ \AA}, \lambda_f = 5577 \text{ \AA}, \text{M} = \text{O}_2$			
4.2	10	32	3.2
7	9	22.3	2.48
14.3	7.0	14.3	2.04
19.8	6.5	6.3	0.97
29.3	5.8	2.0	0.35
38.5	5.0	1.76	0.35
47.3	4.2	1.28	0.3
66.4	3.3	1.0	0.3
$\lambda_i = 4047 \text{ \AA}, \lambda_f = 6300 \text{ \AA}, \text{M} = \text{He}$			
4.8	13	5	0.38
9.2	10.4	2.6	0.25
17	8.0	0.2	0.025
34	4.8	0	0
50	3.8	0	0
$\lambda_i = 4047 \text{ \AA}, \lambda_f = 6300 \text{ \AA}, \text{M} = \text{N}_2$			
5	25	37.5	1.5
11	19	4.8	0.25
17	12.5	3.33	0.26
36	8.75	1.21	0.138
74	4.5	0.06	0.013

TABLE I (continued)

10 <sup>3</sup> [NO <sub>2</sub> ] (Torr)	α (Torr <sup>-1</sup> )	β (Torr <sup>-2</sup> )	β/α(Torr <sup>-1</sup> )
$\lambda_i = 4047 \text{ \AA}, \lambda_f = 6300 \text{ \AA}, M = O_2$			
5	18.2	10.3	0.565
9.5	13.8	5.62	0.41
17	10.5	4.75	0.45
32	8.0	0.77	0.096
48	7.5	0	0.0
68	4.5	0	0.0
$\lambda_i = 4358 \text{ \AA}, \lambda_f = 4860 \text{ \AA}, M = He$			
4.2	16.6 <sup>a</sup>	5.6 <sup>a</sup>	0.34
12	11.8	0.61	0.052
36	5.0	0.125	0.025
75	2.5	0.10	0.04
$\lambda_i = 4358 \text{ \AA}, \lambda_f = 4860 \text{ \AA}, M = N_2$			
3.88	32.5	6.75	0.208
41	7.1	0.635	0.090
80	4.8	0.30	0.062
$\lambda_i = 4358 \text{ \AA}, \lambda_f = 4860 \text{ \AA}, M = O_2$			
5.1	30	90	3.0
11	21.3	9.4	0.44
30	10.6	1.5	0.142
76	5.0	0.75	0.150
$\lambda_i = 4358 \text{ \AA}, \lambda_f = 5577 \text{ \AA}, M = He$			
6	15	—	—
13	10.8	—	—
31	5.6	0.2	0.036
49	4.0	0.16	0.04
71	2.8	0.06	0.02
$\lambda_i = 4358 \text{ \AA}, \lambda_f = 5577 \text{ \AA}, M = N_2$			
8	24	—	—
13	17.4	2.52	0.145
33	8.8	1.2	0.136
47	7.1	0.92	0.130
72	4.6	0.312	0.068
$\lambda_i = 4358 \text{ \AA}, \lambda_f = 5577 \text{ \AA}, M = O_2$			
5	32	—	—
12	19	—	—
28	13.2	2.1	0.16
47	8.0	0.4	0.05
69	5.5	0.18	0.033
$\lambda_i = 4358 \text{ \AA}, \lambda_f = 6300 \text{ \AA}, M = He$			
6	13	—	—
11	10	3.8	0.38
15	10	—	—
26	6.2	0.17	0.03

TABLE I (continued)

$10^6[\text{NO}_2]$ (Torr)	$\alpha$ (Torr <sup>-2</sup> )	$\beta$ (Torr <sup>-2</sup> )	$\beta/\alpha$ (Torr <sup>-1</sup> )
39	4.5	0.125	0.028
49	3.8	0.116	0.03
67	3.2	0.0105	0.003
78	2.4	0.0	0.0
$\lambda_i = 4358 \text{ \AA}, \lambda_f = 6300 \text{ \AA}, \text{M} = \text{N}_2$			
5	23.4	6.6	0.282
14	11.7	2.1	0.179
27	9.8	1.4	0.143
39	8.2	1.06	0.129
53	5.7	0.22	0.04
63	5.5	0.083	0.015
75	3.8	0.0	0.0
$\lambda_i = 4358 \text{ \AA}, \lambda_f = 6300 \text{ \AA}, \text{M} = \text{O}_2$			
6.6	18	—	—
13.9	12.8	1.77	0.138
45	7.2	0.23	0.032
66	4.4	0.06	0.0135
$\lambda_i = 4800 \text{ \AA}, \lambda_f = 5577 \text{ \AA}, \text{M} = \text{He}$			
4.2	20	12.4	0.62
8.8	15	8.3	0.55
20	10.2	3.04	0.30
43	5.7	1.25	0.22
71	3.0	0.16	0.05
$\lambda_i = 4800 \text{ \AA}, \lambda_f = 5577 \text{ \AA}, \text{M} = \text{N}_2$			
5	25	—	—
9.8	18.2	35.2	1.94
24	11.5	4.3	0.374
36.7	10.3	2.62	0.254
71	4.0	1.22	0.305
$\lambda_i = 4800 \text{ \AA}, \lambda_f = 5577 \text{ \AA}, \text{M} = \text{O}_2$			
3.6	25	162	6.5
48	4.6	1.35	0.29
74	3.4	1.18	0.35
$\lambda_i = 4800 \text{ \AA}, \lambda_f = 6300 \text{ \AA}, \text{M} = \text{He}$			
5	15	20	1.33
9	11.7	5.5	0.47
45	5.0	1.2	0.24
56	4.0	0.1	0.025
70	3.0	0.0	0
$\lambda_i = 4800 \text{ \AA}, \lambda_f = 6300 \text{ \AA}, \text{M} = \text{N}_2$			
4.6	25	214	8.6
11	19.2	13.0	0.68
18	12.3	7.8	0.64
36	8.7	1.6	0.18

TABLE I (continued)

10 <sup>3</sup> [NO <sub>2</sub> ] (Torr)	$\alpha$ (Torr <sup>-1</sup> )	$\beta$ (Torr <sup>-2</sup> )	$\beta/\alpha$ (Torr <sup>-1</sup> )
$\lambda_i = 4800 \text{ \AA}, \lambda_f = 6300 \text{ \AA}, M = O_2$			
5	26	31.8	1.22
9.6	23	17.2	0.75
17	9.5	5.25	0.55
40	7.8	1.82	0.23
48	7.5	0.75	0.10
74	4.25	0.62	0.14

<sup>a</sup> Based on [He] < 10 Torr.

#### DISCUSSION

Three studies<sup>2, 8, 9</sup> of the radiative lifetime are in reasonable agreement. Both Neuberger and Duncan<sup>2</sup> and Keyser *et al.*<sup>8</sup> found no dependence of the radiative lifetime with either incident or emitting wavelength. Schwartz and Johnston<sup>9</sup> found about a factor of two change with incident wavelength. However, this is not a significant deviation and may be within the experimental uncertainty. All investigators have concluded that the fluorescence comes from a single electronically excited state, and we concur.

There now exists overwhelming evidence that the fluorescence does not follow a simple one-state Stern–Volmer mechanism. First, the self-quenching Stern–Volmer plot deviates from linearity at NO<sub>2</sub> pressures below 0.005 Torr. Furthermore a red-shift in the emission spectrum occurs as the NO<sub>2</sub> pressure is increased. Second, both the self-quenching and the foreign-gas quenching constants depend on the fluorescence wavelength for a given incident wavelength. This only can be interpreted in terms of different emitting states being involved at the different emitting wavelengths. Third, our work now shows that foreign-gas quenching does not obey the simple Stern–Volmer law. In accordance with the ideas of the Kaufman group<sup>7, 8</sup> and Schwartz and Johnston<sup>9</sup>, fluorescence must be occurring from several vibrational levels of a single electronic state.

The important remaining question is whether the absorbing and emitting electronic states are the same. If the radiative lifetime computed from the integrated absorption coefficient is different from that measured directly, as seems to be the case, then the two electronic states must be different. Douglas<sup>5</sup> argues that the long observed lifetime is due to coupling with vibrational levels of other electronic states. Thus he explains the long lifetime as being due to the ratio of the vibrational degeneracies of the coupled states. Clearly this ratio must be a strong function of both  $\lambda_i$  and  $\lambda_f$ , and the observed radiative lifetime should change markedly with both  $\lambda_i$  and  $\lambda_f$  (perhaps by as much as a factor of 100), contrary to the experimental findings. Thus Douglas' explanation fails.

Sakurai and Broida<sup>10</sup> have pointed out that the radiative lifetime computed from the integrated absorption coefficient could be  $\sim 10^{-5}$  sec, or within a factor of 5 of that observed. This discrepancy still seems too large, but perhaps is within the experimental uncertainty. Thus we shall first consider the possibility now in vogue, *i.e.* the absorbing and emitting electronic states are the same, and show that this possibility also fails for kinetic reasons.

#### *One electronically excited state mechanism*

In order to simplify the discussion we will consider only two vibrational levels,  $\text{NO}_2^*$  and  $\text{NO}_2^{**}$  of the excited electronic level. Thus some quantitative results will represent average values, but the qualitative arguments will be unaffected. The  $\text{NO}_2^*$  state corresponds to the energy level initially formed on absorption. The state  $\text{NO}_2^{**}$  corresponds to lower vibrational levels, more or less the lowest energy levels that can emit at any  $\lambda_f$ . Thus  $\text{NO}_2^{**}$  corresponds to low-lying, but different vibrational levels for the various  $\lambda_f$ . Consequently quenching constants for  $\text{NO}_2^{**}$  are different at different  $\lambda_f$ . The generalized mechanism is:



Fluorescence can occur from both  $\text{NO}_2^*$  and  $\text{NO}_2^{**}$ . The expression for the relative emission yield in the absence of foreign gases,  $Q_0$ , is:

$$\frac{\varepsilon[\text{NO}_2]}{Q_0} = \frac{(k_1 + k_2[\text{NO}_2])(k_4 + k_5[\text{NO}_2])}{k_{1a}(k_4 + k_5[\text{NO}_2]) + k_{4a}k_{2a}[\text{NO}_2]} \quad (IV)$$

where  $k_1 \equiv k_{1a} + k_{1b}$ ,  $k_2 \equiv k_{2a} + k_{2b}$ , *etc.* This expression is not of the Stern-Volmer form, since emission occurs from two states, and conforms to the findings at low  $\text{NO}_2$  pressure<sup>8,9</sup>. However, as the  $\text{NO}_2$  pressure is raised, reaction (1) is rapidly quenched, and eqn. (IV) reduces to:

$$\frac{\varepsilon[\text{NO}_2]}{Q_0} = (k_2/k_{2a}k_{4a})(k_4 + k_5[\text{NO}_2]) \quad (V)$$

which is the Stern-Volmer expression and conforms to Figs. 1 and 2. Since this expression holds for  $[\text{NO}_2] > 0.005$  Torr,  $k_2[\text{NO}_2] \gg k_1$  at this pressure.

Assuming  $k_2 \sim 5 \times 10^{11} M^{-1} \text{sec}^{-1}$ , and since  $k_1 = 2 \times 10^4 \text{ sec}^{-1}$ ,  $k_2[\text{NO}_2]/k_1 = 6.7$  at  $[\text{NO}_2] = 0.005 \text{ Torr}$ . Thus this mechanism is acceptable if reaction (2) proceeds on very collision.

In the presence of foreign gases, the general expression for  $Q$  is:

$$\frac{\varepsilon[\text{NO}_2]}{Q} = \frac{(k_1 + k_2[\text{NO}_2] + k_3[\text{M}]) (k_4 + k_5[\text{NO}_2] + k_6[\text{M}])}{k_{1a}(k_4 + k_5[\text{NO}_2] + k_6[\text{M}]) + k_{4a}(k_{2a}[\text{NO}_2] + k_{3a}[\text{M}])} \quad (\text{VI})$$

but for pressures  $> 0.005 \text{ Torr}$ , reaction (1) is quenched and eqn. (VI) reduces to:

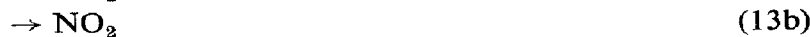
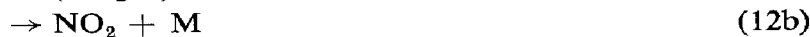
$$\frac{\varepsilon[\text{NO}_2]}{Q} = \frac{(k_2[\text{NO}_2] + k_3[\text{M}]) (k_4 + k_5[\text{NO}_2] + k_6[\text{M}])}{k_{4a}(k_{2a}[\text{NO}_2] + k_{3a}[\text{M}])} \quad (\text{VII})$$

Now the ratio  $Q_0/Q$  must satisfy eqn. (III) in order to fit the experimental facts. This will only be the case if  $k_{3a}[\text{M}] \ll k_{2a}[\text{NO}_2]$  and if either  $k_3[\text{M}] \ll k_2[\text{NO}_2]$  or  $k_6[\text{M}] \ll k_5[\text{NO}_2]$ . In the former case, upper vibrational levels are extremely efficiently quenched by NO<sub>2</sub>, but not by M, whereas the lower vibrational levels are quenched equally or more efficiently by M than NO<sub>2</sub>. In the latter case the reverse is so but  $k_{3a}[\text{M}]$  must still be negligible compared to  $k_{2a}[\text{NO}_2]$ . In either case it is difficult to understand the inversion in quenching efficiency between NO<sub>2</sub> and M as a function of vibrational level. On this basis, we conclude that the one electronic state mechanism cannot be operative.

### Two electronically excited state mechanism

It is our conviction that the electronically absorbing and emitting states must be different. Presumably the absorbing state is <sup>2</sup>B<sub>1</sub> as shown by Douglas and Huber<sup>14</sup>, whereas the emitting state is <sup>2</sup>B<sub>2</sub>, as shown by Abe *et al.*<sup>16</sup>.

The two vibrational level simplification of the mechanism we envisage is:



where  $\text{NO}_2^*$  is the electronic state produced by light absorption,  $(\text{NO}_2^{**})_n$  is a highly vibrationally excited level of the emitting electronic state, and  $(\text{NO}_2^{**})_m$  represents low-lying vibrational levels of the emitting electronic state. The energies of  $\text{NO}_2^*$  and  $(\text{NO}_2^{**})_n$  are the same, whereas the lower lying  $(\text{NO}_2^{**})_m$  is the lowest lying energy level that can emit at any  $\lambda_f$ ; thus  $(\text{NO}_2^{**})_m$  is different at different  $\lambda_f$  even if  $\lambda_i$  is the same.

Emission from  $(\text{NO}_2^{**})_n$  accounts for the deviation in the Stern–Volmer plots below 0.005 Torr pressure. Under our conditions it is negligible, and reaction (10) can be ignored.

The rate constant for reaction (7) must be considerably larger than that for radiation of  $\text{NO}_2^*$  ( $\lesssim 4 \times 10^6 \text{ sec}^{-1}$ ). Thus  $k_7$  is almost surely  $> 10^7 \text{ sec}^{-1}$ . Since  $k_8$  cannot be greater than collision frequency, *i.e.*  $\sim 5 \times 10^{11} \text{ M}^{-1} \text{ sec}^{-1}$ , reaction (8) is always negligible at our  $\text{NO}_2$  pressures ( $< 0.080$  Torr).

The mechanism leads to a complex rate law. For simplicity we assume that  $k_{11a}/k_{11} = k_{12a}/k_{12} = \gamma$ . This simplification is not required for the mechanism to be valid, but it does reduce mathematical manipulations. With this simplification, and neglecting reactions (8) and (10), the rate law in the absence of M becomes:

$$\gamma \varepsilon [\text{NO}_2]/Q_0 = k_7(k_{13} + k_{14}[\text{NO}_2])/k_{7a}k_{13a} \quad (\text{VIII})$$

Plots of  $[\text{NO}_2]/Q_0$  vs.  $[\text{NO}_2]$  are shown in Figs. 1 and 2, and they are linear as predicted by eqn. (VIII). The ratio of slope to intercept gives  $k_{14}/k_{13}$ , and these values are listed in Table II for each  $\lambda_i$  and  $\lambda_f$ . They range from 60 to 175 Torr<sup>-1</sup>, the values increasing with  $\lambda_i$ .

TABLE II  
RATE CONSTANT RATIOS

M	$k_{14}/k_{13}$ (Torr <sup>-1</sup> )	$k_{14}/k_{15}$	$k_{18}/k_{15}$ (Torr)	Source
$\lambda_i = 4047 \text{ \AA}, \lambda_f = 5577 \text{ \AA}$				
None	60	—	—	Eqn. (VIII), Fig. 1
He	44	5.0	0.11	Eqn. (X), Fig. 9
N <sub>2</sub>	36	3.4	0.055	Eqn. (X), Fig. 10
O <sub>2</sub>	43	3.4	0.08	Eqn. (X), Fig. 11
—	~ 110			Keyser <i>et al.</i> <sup>8</sup>
$\lambda_i = 4047 \text{ \AA}, \lambda_f = 6300 \text{ \AA}$				
None	73	—	—	Eqn. (VIII), Fig. 1
He	67	4.15	0.063	Eqn. (X), Fig. 9
N <sub>2</sub>	66	2.58	0.046	Eqn. (X), Fig. 10
O <sub>2</sub>	56	2.5	0.038	Eqn. (X), Fig. 11
—	~ 75			Keyser <i>et al.</i> <sup>8</sup>

TABLE II (continued)

M	$k_{14}/k_{13}$ (Torr <sup>-1</sup> )	$k_{14}/k_{15}$	$k_{13}/k_{15}$ (Torr)	Source
$\lambda_i = 4358 \text{ \AA}, \lambda_f = 4860 \text{ \AA}$				
None	140	—	—	Eqn. (VIII), Fig. 1
He	116	4.65	0.04	Eqn. (X), Fig. 9
N <sub>2</sub>	133	2.66	0.02	Eqn. (X), Fig. 10
O <sub>2</sub>	120	2.4	0.02	Eqn. (X), Fig. 11
—	~ 200			Keyser <i>et al.</i> <sup>8</sup>
—	~ 130			Myers <i>et al.</i> <sup>7</sup>
$\lambda_i = 4358 \text{ \AA}, \lambda_f = 5577 \text{ \AA}$				
None	103	—	—	Eqn. (VIII), Fig. 1
He	110	4.4	0.04	Eqn. (X), Fig. 9
N <sub>2</sub>	110	2.65	0.024	Eqn. (X), Fig. 10
O <sub>2</sub>	115	2.3	0.02	Eqn. (X), Fig. 11
—	~ 120			Keyser <i>et al.</i> <sup>8</sup>
—	~ 70			Myers <i>et al.</i> <sup>7</sup>
$\lambda_i = 4358 \text{ \AA}, \lambda_f = 6300 \text{ \AA}$				
None	91	—	—	Eqn. (VIII), Fig. 2
He	86	4.3	0.05	Eqn. (X), Fig. 9
N <sub>2</sub>	93	2.8	0.03	Eqn. (X), Fig. 10
O <sub>2</sub>	95	2.83	0.03	Eqn. (X), Fig. 11
—	~ 80			Keyser <i>et al.</i> <sup>8</sup>
—	50			Myers <i>et al.</i> <sup>7</sup>
$\lambda_i = 4800 \text{ \AA}, \lambda_f = 5577 \text{ \AA}$				
None	175	—	—	Eqn. (VIII), Fig. 2
He	180	4.15	0.023	Eqn. (X), Fig. 9
N <sub>2</sub>	190	3.42	0.018	Eqn. (X), Fig. 10
O <sub>2</sub>	146	3.8	0.025	Eqn. (X), Fig. 11
$\lambda_i = 4800 \text{ \AA}, \lambda_f = 6300 \text{ \AA}$				
None	140	—	—	Eqn. (VIII), Fig. 2
He	150	4.25	0.028	Eqn. (X), Fig. 9
N <sub>2</sub>	115	2.8	0.024	Eqn. (X), Fig. 10
O <sub>2</sub>	141	2.82	0.02	Eqn. (X), Fig. 11

In the presence of a foreign gas the rate law becomes:

$$\frac{(Q_0/Q-1)}{[M]} = \frac{k_{15}}{k_{13} + k_{14}[\text{NO}_2]} + \frac{k_9}{k_7} + \frac{k_9 k_{15} [M]}{k_7 (k_{13} + k_{14}[\text{NO}_2])} \quad (\text{IX})$$

Equation (IX) has the same form as eqn. (III), and thus conforms to the experimental results with:

$$\alpha = \frac{k_{15}}{k_{13} + k_{14}[\text{NO}_2]} + \frac{k_9}{k_7}$$

$$\beta = \frac{k_9 k_{15}}{k_7 (k_{13} + k_{14}[\text{NO}_2])}$$

If  $k_9/k_7$  is negligible compared to  $k_{15}/(k_{13} + k_{14}[\text{NO}_2])$ , then:

$$\alpha^{-1} = (k_{13} + k_{14}[\text{NO}_2])/k_{15}$$

and plots of  $\alpha^{-1}$  vs.  $[\text{NO}_2]$  should be linear. Such plots are shown in Figs. 9–11, and they are linear in every case. The intercepts give  $k_{13}/k_{15}$ , the slopes give  $k_{14}/k_{15}$ , and the ratio of slope to intercept gives  $k_{14}/k_{13}$ . These values are tabulated in Table II for each  $\lambda_i$  and  $\lambda_f$ .

The values for  $k_{14}/k_{13}$  obtained from the foreign-gas quenching experiments agree well with each other and with the values obtained from the  $\text{NO}_2$  self-quenching experiments. Furthermore they also agree reasonably well with the values obtained in Kaufman's laboratory (also listed in Table II), except for  $\lambda_i = 4047 \text{ \AA}$  and  $\lambda_f = 5577 \text{ \AA}$ . Even here the discrepancy is only about a factor of 2–3. Since

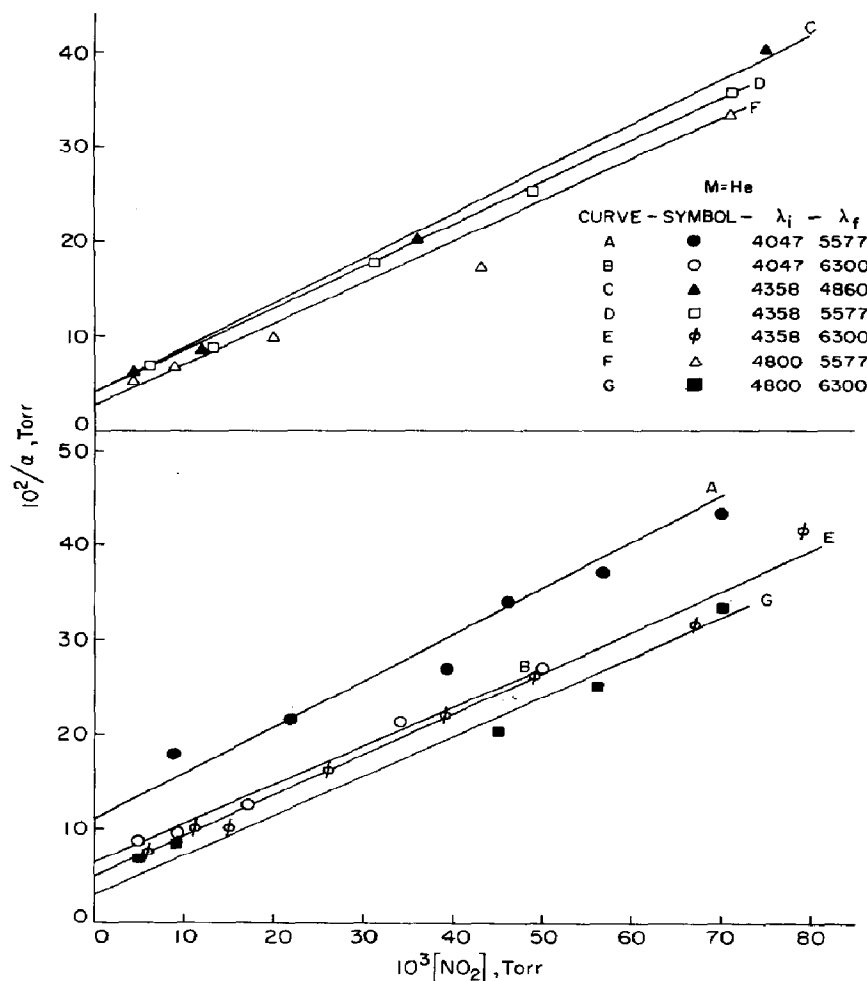


Fig. 9. Plots of  $\alpha^{-1}$  vs.  $[\text{NO}_2]$  at various  $\lambda_i$  and  $\lambda_f$  for the emission of  $\text{NO}_2$  in the presence of He at  $25^\circ\text{C}$ .

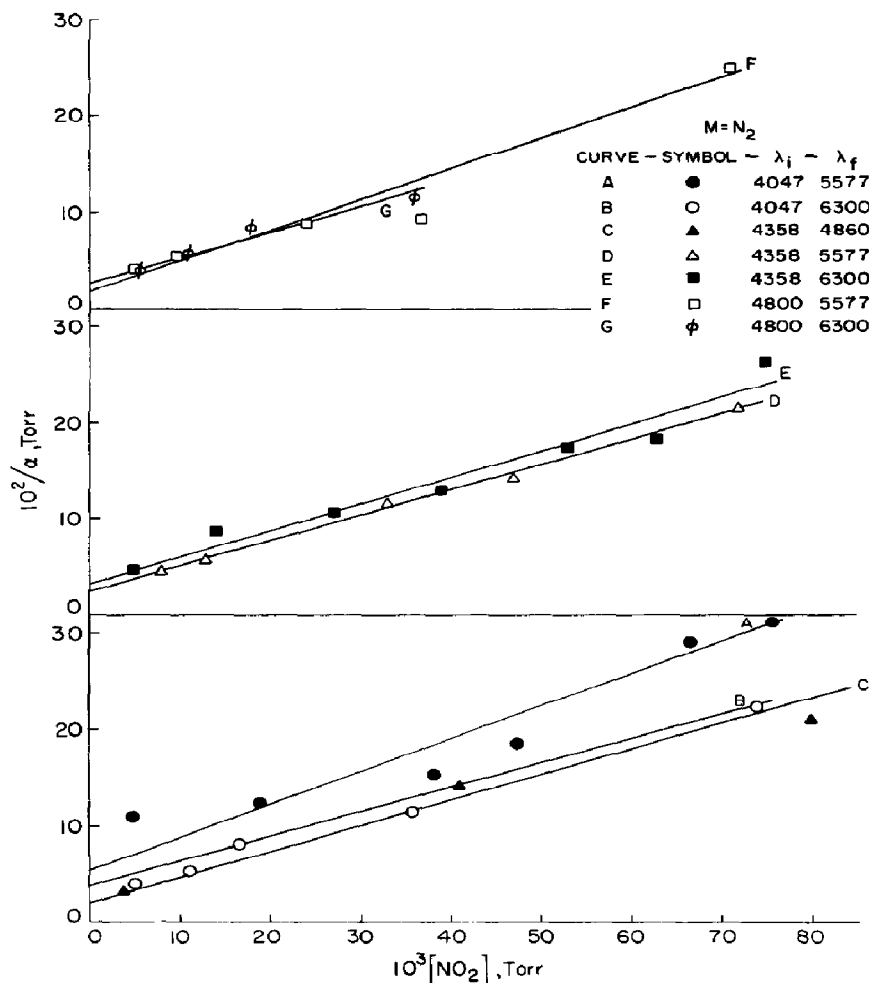


Fig. 10. Plots of  $\alpha^{-1}$  vs.  $[\text{NO}_2]$  at various  $\lambda_i$  and  $\lambda_f$  for the emission of  $\text{NO}_2$  in the presence of  $\text{N}_2$  at 25°C.

$k_{13} \sim 2 \times 10^4 \text{ sec}^{-1}$  and  $k_{14}/k_{13} \sim 100 \text{ Torr}^{-1}$ ,  $k_{14} \sim 4 \times 10^{10} \text{ M}^{-1} \text{ sec}^{-1}$  which corresponds to deactivation about once in every 10 collisions.

The ratio  $k_{14}/k_{15}$  gives the relative efficiency of  $\text{NO}_2$  and M as quenching gases for  $(\text{NO}_2^{**})_m$ . The relative efficiencies are about the same at all  $\lambda_i$  and  $\lambda_f$  and follow the trend expected, i.e. the efficiency increases with molecular complexity. Thus the relative efficiencies are about 0.22/0.35/0.35/1.00 for He,  $\text{N}_2$ ,  $\text{O}_2$ , and  $\text{NO}_2$  respectively in good agreement with the values of 0.29/0.44/0.48/1.00 found by Myers *et al.*<sup>7</sup> Our results also agree with those of Baxter<sup>6</sup> who found the quenching efficiencies to be 0.42/0.33/1.00 for  $\text{N}_2$ ,  $\text{O}_2$ , and  $\text{NO}_2$ , respectively.

The ratio  $\beta/\alpha$  should give  $k_9/k_7$ . These values are listed in Table I for each  $\text{NO}_2$  pressure at each  $\lambda_i$  and  $\lambda_f$ . First it should be noticed that in every case

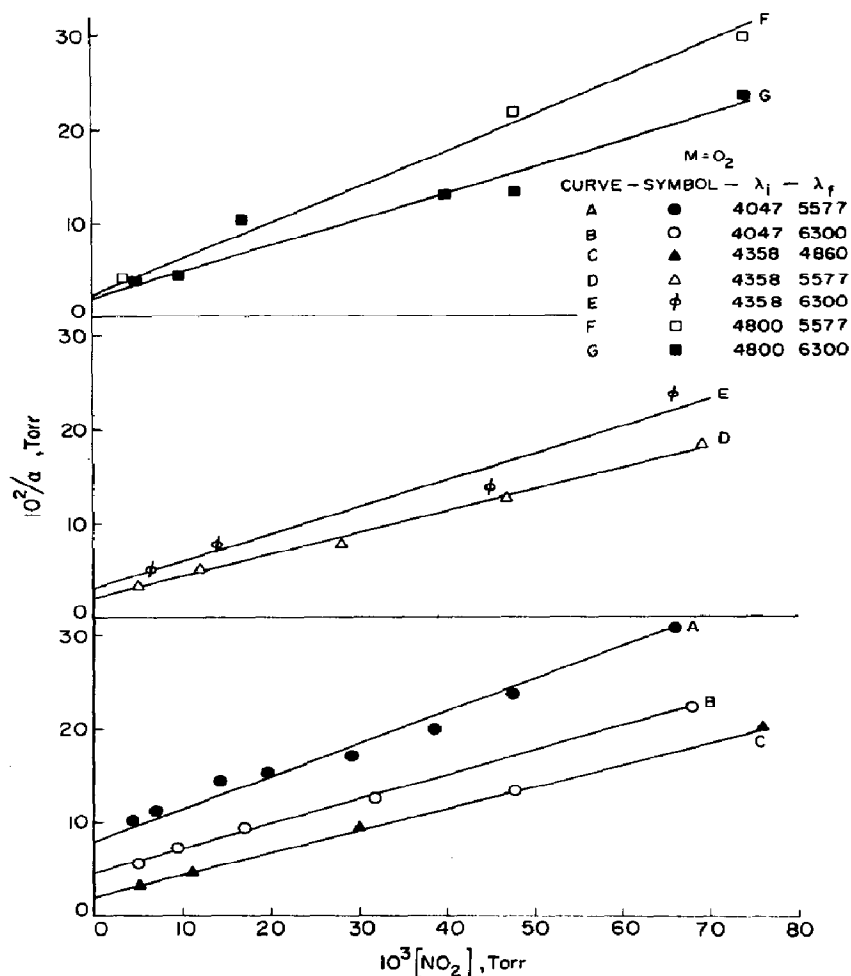


Fig. 11. Plots of  $\alpha^{-1}$  vs.  $[\text{NO}_2]$  at various  $\lambda_i$  and  $\lambda_f$  for the emission of  $\text{NO}_2$  in the presence of  $\text{O}_2$  at  $25^\circ\text{C}$ .

$\beta/\alpha \ll \alpha$ , i.e.  $k_9/k_7 \ll k_{15}/(k_{13} + k_{14}[\text{NO}_2])$ , as assumed earlier. In the worst case  $\beta/\alpha \sim 0.25\alpha$ , but usually  $\beta/\alpha < 0.1\alpha$  and often very much less.

However,  $\beta/\alpha$  is not a constant independent of  $[\text{NO}_2]$  as expected. In fact  $\beta/\alpha$  drops as  $[\text{NO}_2]$  increases at every  $\lambda_i$  and  $\lambda_f$ . Thus either  $k_9$  or  $k_7$  or both has some functional dependence on  $[\text{NO}_2]$ . It cannot be  $k_7$ , for then linear Stern-Volmer plots would not have been obtained for self-quenching in the absence of foreign gases. Thus  $k_9$  must be a complex reaction. Since  $k_7 > 10^{-7} \text{ sec}^{-1}$  and  $k_9/k_7 \sim 1 \text{ Torr}^{-1}$ ,  $k_9 \geq 10^{11} \text{ M}^{-1} \text{ sec}^{-1}$ ; reaction (9) is a very efficient quenching reaction. Perhaps it involves quenching to even a third electronic state (a quartet?) which can emit radiation. At present we have no explanation for this anomaly, but it together with the deviation from linearity of Fig. 6 at very high He pressure

suggest that even two excited electronic states may not be sufficient to explain the photophysical processes accompanying light absorption by NO<sub>2</sub>.

#### ACKNOWLEDGEMENT

We wish to thank Professors John Nisbet and Leslie Hale for their help in designing the electronic equipment. This work was supported by the National Aeronautics and Space Administration through Grant No. NGL-009-003 for which we are grateful.

#### REFERENCES

- 1 R. G. W. Norrish, *J. Chem. Soc.*, (1929) 1611.
- 2 D. Neuberger and A. B. F. Duncan, *J. Chem. Phys.*, 22 (1954) 1693.
- 3 T. C. Hall, Jr. and F. E. Blacet, *J. Chem. Phys.*, 20 (1952) 1745.
- 4 J. K. Dixon, *J. Chem. Phys.*, 8 (1940) 157.
- 5 A. E. Douglas, *J. Chem. Phys.*, 45 (1966) 1007.
- 6 W. P. Baxter, *J. Am. Chem. Soc.*, 52 (1930) 3920.
- 7 G. H. Myers, D. M. Silver and F. Kaufman, *J. Chem. Phys.*, 44 (1966) 718.
- 8 L. F. Keyser, S. Z. Levine and F. Kaufman, *J. Chem. Phys.*, 54 (1971) 355.
- 9 S. E. Schwartz and H. S. Johnston, *J. Chem. Phys.*, 51 (1969) 1286.
- 10 K. Sakurai and H. P. Broida, *J. Chem. Phys.*, 50 (1969) 2404.
- 11 W. H. Fink, *J. Chem. Phys.*, 54 (1971) 2911.
- 12 R. A. Gangi and L. Burnelle, *J. Chem. Phys.*, 55 (1971) 843.
- 13 R. A. Gangi and L. Burnelle, *J. Chem. Phys.*, 55 (1971) 851.
- 14 A. E. Douglas and K. P. Huber, *Can. J. Phys.*, 43 (1965) 74.
- 15 P. B. Sackett and J. T. Yardley, *J. Chem. Phys.*, 57 (1972) 152.
- 16 K. Abe, F. Myers, T. K. McCubbin and S. R. Polo, *J. Mol. Spectros.*, 38 (1971) 552.